Article

No longer in doubt: Discovery of a second specimen corroborates the validity of *Anolis incredulus* Garrido and Moreno 1998 (Reptilia, Iguania)

KEVIN DE QUEIROZ[1*], JONATHAN M. HUIE[1,2] & ESTHER M. LANGAN[1]

[1]*Department of Vertebrate Zoology, National Museum of Natural History, Smithsonian Institution, 10th St and Constitution Ave NW, Washington DC 20560, USA.*
✉ *dequeirozk@si.edu;* 🔵 *https://orcid.org/0000-0001-9165-3522*
✉ *langane@si.edu;* 🔵 *https://orcid.org/0009-0006-1989-9839*
[2]*Department of Biological Sciences, The George Washington University, Washington, DC 20052, USA.*
✉ *jonathanmhuie@gmail.com;* 🔵 *https://orcid.org/0000-0002-7925-7372*
*Corresponding author. ✉ *dequeirozk@si.edu*

Abstract

The species *Anolis incredulus* was proposed based on a single, poorly preserved specimen from the Sierra Maestra (mountain range) of southeastern Cuba. As its name suggests, this species was considered likely to raise doubts when it was first proposed, and it has been explicitly treated by some recent authors as a *species inquirenda* (a species of doubtful identity). Here we report on a second specimen of *Anolis incredulus* discovered in the amphibian and reptile collection of the National Museum of Natural History (Smithsonian Institution) that was collected more than 100 years before the holotype. We describe this specimen in detail and compare it both with the description of the holotype of *A. incredulus* and with presumed closely related Cuban species, providing evidence that it matches closely with the former and is distinct from the latter, thus corroborating the status of *A. incredulus* as a valid species. We also score and measure the specimen for sets of morphological characters to make inferences about its phylogenetic relationships and ecology (structural habitat use). Our results indicate that *Anolis incredulus* is likely a member of a clade of mostly Cuban twig-anole species and that it is a member of the twig ecomorph category, although its reported green coloration suggests either an erroneous ecomorph assignment or a difference in color from that of most other species of Cuban twig anoles.

Key words: *Anolis angusticeps, Anolis isolepis*, *Anolis guazuma*, Cuba, ecological morphology, *species inquirenda*, phylogenetic relationships

Introduction

In July of 1963, Gerardo Albañir, a member of an entomological expedition to Pico Turquino in the Sierra Maestra of eastern Cuba, collected a small, gravid, female lizard, which was deposited in the collection of the director of the Museo Cubano de Ciencias Naturales, Miguel L. Jaume (Garrido & Moreno 1998). Twenty years later, Garrido (1983) mentioned this specimen in the paper in which he proposed the new species *Anolis guazuma*, noting differences between the Albañir specimen and female *A. angusticeps*, and providing measurements and scale counts for it along with comparable data for *A. guazuma* and *A. angusticeps*. He chose not to name a new species for the specimen at that time in the hopes of obtaining additional specimens from future expeditions. However, when no additional specimens had been obtained after fifteen more years, Garrido & Moreno (1998) decided to name the species in the hopes that this act would inspire others to search for additional specimens. They named the species *Anolis incredulus*, "por las dudas que pudiera acarrear" [for any doubts that might arise] (p. 39). And doubts did arise. Most notably, the species was not included in the study of "all extant species of *Anolis*" by Poe *et al.* (2017), and more recently, owing to the poor condition of the only known specimen, Díaz *et al.* (2022) concluded that it was appropriate to consider *A. incredulus* a *species inquirenda*—a species of doubtful identity needing further investigation (ICZN 1999).

In June 2018, while processing a loan request for specimens of *Anolis* lizards for a series of studies on the locomotor

skeleton of this group (Fiener *et al.* 2020, 2021a, b), one of us (EML) noticed that the specimens identified as *A. guazuma* in the amphibian and reptile collection of the National Museum of Natural History (NMNH), Smithsonian Institution, appeared to represent two different species. This suspicion was confirmed by KdQ, who eventually reached the conclusion that one specimen, USNM 5095, which differed markedly from the others, likely represents a second specimen of *A. incredulus.* That inference was based on the general agreement between the scalation of USNM 5095 and the description provided for *A. incredulus*, as well as that the USNM specimen exhibited evidence that it may have been green in life, a characteristic reported for the holotype of *A. incredulus* (Garrido & Moreno 1998) and an important difference between that species and species of Cuban twig anoles such as *A. guazuma* and *A. angusticeps*. It is also a similarity to *Anolis isolepis* and its close relatives, to which *A. incredulus* has previously been compared (Garrido & Moreno 1998; Garrido & Hedges 2001).

Because of the importance of USNM 5095 in corroborating *Anolis incredulus* as a valid species, we here provide a detailed description of this specimen. We compare it with the original description of *A. incredulus* as well as with members of the *Anolis angusticeps* and *Anolis isolepis* species groups to provide evidence that it corresponds closely to the former and differs markedly from the latter. We also perform analyses to make inferences about the phylogenetic relationships and ecology (structural habitat use) of this still poorly known species.

Materials and methods

Specimens examined. In addition to USNM 5095, we examined specimens of the following species from the collection of the Division of Amphibians and Reptiles at the National Museum of Natural History: *A. angusticeps* (USNM 497987, 497990, 497991, 497993, 497996), *A. guazuma* (USNM 589688, 589689, 589690, 589691, 589692), *A. isolepis* (USNM 538870, 538871, 589699, 589700, 589701), *A. altitudinalis* (USNM 538873, 538874), and *A. porcatus* (USNM 314415–314416). Note that although the current name of the museum in which these specimens are housed is the National Museum of Natural History (NMNH), the standard acronym used to refer to specimens in the collection of Division of Amphibians and Reptiles is "USNM" (Sabaj 2020), based on the earlier name United States National Museum. Because of the poor condition of the holotype of *Anolis incredulus* and the difficulties of shipping specimens between the United States and Cuba, we did not examine the holotype of *A. incredulus* directly, although photographs were provided by Manuel Iturriaga and others have been published by Díaz *et al.* (2022).

External morphology. The external morphology of USNM 5095 was examined with the aid of a Zeiss SV8 stereo dissecting microscope. Our descriptions of external morphology emphasize standard characters that have been used in anole taxonomy (Williams 1995; Köhler 2014). Some measurements were taken with an ocular micrometer, others with digital calipers.

Skeletal morphology. Skeletal morphology was examined using micro-computed tomography (μCT). USNM 5095 and one specimen each of *Anolis guazuma* (USNM 589689), *A. altitudinalis* (USNM 538874), and *A. isolepis* (USNM 589700) were scanned using the GE Phoenix v|tome| x M 240/180kV Dual Tube μCT system in the Scientific Imaging Laboratory at the Smithsonian Institution's National Museum of Natural History (resolution = 39.5–48.6 μm, 80–90 kV, 170 μA). The CT data files were imported into 3D Slicer (Version 5.0.2, Kikinis *et al.* 2014) and visualized with the SlicerMorph toolkit (Rolfe *et al.* 2021). Our descriptions of skeletal morphology emphasize standard characters that have been used in anole systematics (Etheridge 1959; Poe 1998, 2004).

Phylogenetics. We scored *Anolis incredulus*, based on USNM 5095 and data from the published description of the holotype (Garrido & Moreno 1998), for the set of morphological characters used by Poe *et al.* (2017) in a comprehensive study of anole phylogeny. We then added *A. incredulus* to the dataset of Poe *et al.* (2017) and analyzed a subset of the species (justified below based on our data for USNM 5095) using Bayesian phylogenetic inference, implemented with MrBayes version 3.2.7 (Ronquist *et al.* 2012). We used the same models and priors as those used by Poe *et al.* (2017), except that the temperature parameter for Metropolis coupling was set to 0.01 rather than 0.001 and no time calibration was used. Consequently, the nodes in our phylogram (inferred under a relaxed-clock model) reflect relative divergence times but are otherwise undated.

Ecological morphology. Specimens of *A. incredulus* (USNM 5095), *A. altitudinalis* (USNM 538873), *A. guazuma* (USNM 589689), and *A. isolepis* (USNM 538870, 538871) were measured using digital calipers for the set of morphological characters used by Huie *et al.* (2021) in a broadly comparative study of anole ecological

morphology (*A. isolepis* was included in that study as a previously unclassified species, while *A. angusticeps* was included in that study as a predetermined twig anole species). The characters measured were snout-vent length (SVL), tail length, head length, snout length, head width, humerus length, radius length, hand length, femur length, tibia length, foot length and width of the subdigital pads on digit IV of both manus and pes. Unlike Huie *et al.* (2021), we also included lamella counts for both manual and pedal digit IV. The four species were then added to the dataset of 71 Caribbean ecomorph species (species with sufficient ecological and morphological data to support ecomorph assignments as assumptions of the analysis) of Huie *et al.* (2021). All traits were log-transformed and phylogenetically regressed against SVL, and the residuals were used as size-corrected variables. The four species were then assessed for ecomorph assignment using a subset of the methods used by Huie *et al.* (2021), namely phylogenetically informed principal components analysis (pPCA), discriminant function analysis (DFA) trained with the ecomorph species, and three distance criteria based on Euclidean distances derived from the pPCA (see Table 2 for details). For the phylogenetic corrections, *A. incredulus* was inserted into the maximum clade credibility tree of Poe *et al.* (2017) where it was placed in the results of our phylogenetic analysis. Because USNM 5095 has a regenerated tail, the analyses were performed excluding tail length, although a separate analysis was performed for the other three species including tail length. In addition, analyses using standard (non-phylogenetic) PCA were also performed to assess whether incorporation of the phylogenetic information had a strong effect on predicted ecomorph assignment.

FIGURE 1. USNM 5095, inferred to be a second specimen of *Anolis incredulus,* in dorsal (above) and ventral (below) views. Note bluish iridescence in the temporal region.

The Specimen (Fig. 1). The specimen designated USNM 5095 (Fig. 1) was collected more than 100 years before the holotype of *A. incredulus* was collected but has been largely overlooked for most of its existence. According to the hand-written entry and annotations in the catalogue ledger, that number originally designated a lot of 7 specimens that was catalogued into what is now the NMNH collection on February 1, 1861 and identified (or at least entered in ink) only as *Anolis*. Three of the seven specimens were later identified as *Anolis porcatus* and two as *Xiphocercus valencienni* and re-catalogued with individual numbers. Still later, the specimens identified as *X. valencienni* were reidentified as *A. porcatus* (by E. E. Williams). One of the specimens is not accounted for, and the last remaining specimen associated with the number 5095 was at some unknown time identified as *Anolis isolepis* (in pencil) and later (1998) reidentified as *A. guazuma*. Unfortunately, the locality data are imprecise; they are given only as "Cuba \\ W. I." However, the specimens were collected by the botanical collector Charles Wright, whose travels in Cuba have been documented by Underwood (1905) and Howard (1988). According to those authors, Wright visited several localities in the Sierra Maestra west of Santiago de Cuba (city) prior to February 1861, including Cobre, Nima Nima, and San Juan de Buenavista, as well as other localities to the east of Santiago de Cuba in the Cordillera de la Gran Piedra. The type locality of *Anolis incredulus*, Pico Turquino, is in the western Sierra Maestra. Thus, what little is known about the provenance of USNM 5095 allows for the possibility that it was collected in the same mountain range as type (and only known) locality for *A. incredulus*.

Description of the specimen

External morphology (Fig. 2)

To facilitate comparisons, we will present descriptions of the standard characters described by Williams (1995) and by Köhler (2014) separately despite the partial redundancy.

Characters of Williams (1995). 1. Head scales: Most head scales smooth, although the largest scales of the supraorbital semicircles are rugose. 2. Scales between second canthals: ten. 3. Postrostrals: four. 4. Nasal: a divided anterior nasal. Additionally, the nostril is longer than tall and lies in a trough between the canthal and frontal ridges. One scale separates the nasal from the supralabials. 5. Scales between nasal and rostral: two. 6. Scales between supraorbital semicircles: one. 7. Enlarged scales in supraocular disk: two (each side). 8. Elongate superciliaries: one, only slightly enlarged. 9. Superciliary series: composed of small scales that are only slightly larger than adjacent (granular) scales. 10. Loreal rows: four (each side). 11. Loreal number: twenty-two (each side). 12. Interparietal relative to ear: interparietal ca. five times larger than ear opening (by area). 13. Scales between interparietal and semicircles: zero; the interparietal barely contacts the supraorbital semicircles at its anterolateral corners. 14. Scales between interparietal and nape scales: three–four distinctly enlarged + one slightly enlarged scales. 15. Scale rows between suboculars and supralabials: zero; the suboculars and supralabials are in contact. 16. Supralabials to below center of eye: eight (left) seven-eight (right, on border between scales). 17. Postmentals: six. 18. Sublabials: one large sublabial (the first) on each side, followed by a series gradually decreasing in size. 19. Sublabials in contact with infralabials: one (each side); only the first sublabial is in contact with the infralabials. 20. Dorsals: smooth and only slightly raised, granular. 21. Enlarged middorsal rows: two, only slightly enlarged. 22. Middorsal crests: absent. 23. Flank scales: juxtaposed (non-overlapping), homogeneous. 24. Size of ventrals relative to dorsals: ventrals larger than dorsals. 25. Smooth/keeled ventrals: smooth (unkeeled). 26. Ventrals: juxtaposed (non-overlapping). 27. Toe pads: well-developed with pad overlapping second (penultimate) phalanx (incorrectly described by Williams (1995) as overlapping the first phalanx, but the first (ultimate, terminal, ungual) phalanx is small and mostly invested by the claw). 28. Lamellar number: twenty on the right side under the third- and fourth-most distal phalanges (incorrectly designated by Williams (1995) as phalanges 2 and 3). The left side appears to have a developmental abnormality; it lacks the expanded part of the pad as well as the entire ultimate and penultimate and most of the antepenultimate phalanges. 29. Supradigitals: smooth. 30. Tail: strongly compressed; the height is greater than twice the width at the 17th caudal vertebra. 31. Tail crest: none; scales of middorsal row not raised to form a crest. 32. Postanals: absent, no enlarged postcloacal scales. 33. Dewlap (male): large, extends well posterior to insertion of forelimbs. 34. Dewlap (female) not applicable (small in the female holotype of *A. incredulus*). 35. Snout-vent [maximum] (male): 46.0 mm (measured to nearest 0.5 mm). 36. Snout-Vent [maximum] (female): not applicable (34 mm in the female holotype of *A. incredulus*). 37. Tail length/body length: The tail was measured as 44.5 mm (to nearest 0.5 mm), but it is regenerated. Based on the amount of regeneration (the tail appears almost fully regenerated), the tail length would

probably have been < 55 mm if entire. If so, the tail length to SVL ratio was likely less than 1.2 (55/46 = 1.2), which would be in the shortest category recognized by Williams (1995).
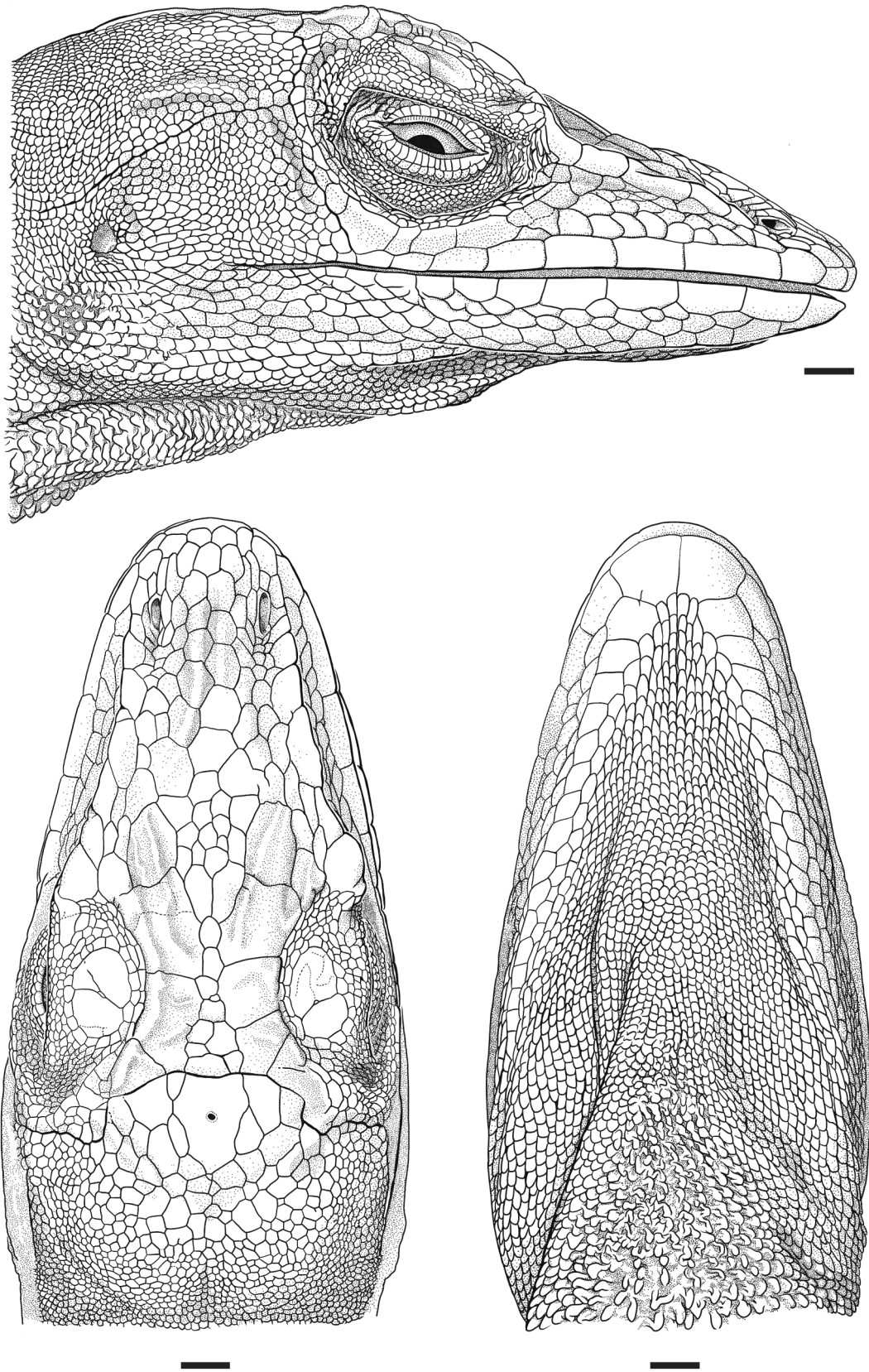

FIGURE 2. Line drawings of the head scales of USNM 5095 in lateral (top), dorsal (lower left), and ventral (lower right) views. Scale bar = 1 mm.

Characters of Köhler (2014). For these characters, SVL is measured to the nearest 0.5 mm, most other measurements to the nearest 0.1 mm, scale sizes to the nearest 0.05. Snout-vent length (SVL): 46.0 mm; small category (<50mm). Tail length (TL): not applicable (tail regenerated), but probably < 55 mm (see Williams character 37). Tail diameter: horizontal diameter of tail (HDT) = 2.0 mm, vertical diameter of tail (VDT) = 2.8 mm at point reached by the heel of the extended leg, although the difference is greater (the tail is more compressed) more posteriorly (see Williams character 30). Shank length (ShL): 7.9 mm. Axilla-groin distance (AGD): 17.8 mm. Diameter of external ear opening: longitudinal diameter of ear (LDE) = 0.5 mm, vertical diameter of ear (VDE) = 0.5 mm; thus, the ear opening is more or less round. Diameter of parietal scale: longitudinal diameter of parietal (LDP) = 1.9 mm, transverse diameter of parietal (TDP) = 1.4 mm. Head length (HL): 14.1 mm. Head width (HW): 7.5 mm. Snout length (SL): 6.8 mm. Postcloacal scale width (PCW): not measured as there are no enlarged postcloacal scales (see Williams character 32). Subdigital pad width (SPW): 0.9 mm. Relative hind limb length (RHLL): The point reached by the tip of the fourth toe when the leg is extended and adpressed to the body was not determined to prevent damage to the specimen. However, the results of our ecomorphological analysis (below) indicate that the specimen has short limbs for its body size.

Number of fourth toe lamellae (ToeLam): 30 (Note that this count is for the proximal three phalanges and thus differs from Williams character 28, which is for the distal two of the proximal three phalanges.). Condition of supradigital scales (CSD): smooth (see Williams character 29). Number of scales between first canthals (1Canths): seven. Number of scales between second canthals (2Canths): 10 (see Williams character 2). Circumnasal condition: Circumnasal (nasal) separated from rostral by two scales (CNS) (Williams character 5) and from first supralabial by one scale (see Williams character 4). Prenasal condition: Two prenasals, neither reaching the upper level of the nostril and both separated from both the rostral and the first supralabial (PNS). Condition of superciliary scales: a single slightly enlarged superciliary (Williams character 8). Number of enlarged supraocular scales (ESO): two greatly enlarged supraoculars on each side (Williams character 7). Condition of supraocular scales (CSO): smooth. Number of supralabial scales to level below center of eye (SPLeye): eight (left) seven-eight (right, on border between scales) (Williams character 16). Number of infralabial scales to level below center of eye (IFLeye): seven (each side; the right is close to seven-eight border). Number of postmental scales (PM): six (Williams character 17), the outer ones greatly enlarged.

Number of sublabial scales (SubL): one enlarged sublabial (each side, the outer postmental) in contact with the infralabials, the rest separated from the infralabials by one or more scales and gradually decreasing in size posteriorly (Williams characters 18 and 19). Number of postrostral scales (PR): four (Williams character 3). Number of internasal scales (IN): six. Condition of snout scales (CSS): unkeeled, some slightly raised, those that overlie the borders of the prefrontal depression rugose. Condition of prefrontal depression (PFDep): very distinct, especially for a lizard of this size. Condition of parietal depression (PDep): very distinct, especially for a lizard of this size. Condition of canthal ridge (CR): very distinct, and somewhat elevated vertically. Number of scales between supraorbital semicircles (IO): one (Williams character 6). Number of scales between supraorbital semicircles and interparietal plate (IP/IO): zero; the interparietal barely contacts the supraorbital semicircles at its anterolateral corners (Williams character 13). Size of scales adjacent to interparietal plate (ScIP): interparietal at least two times larger than adjacent scales, except for those of the supraorbital semicircles. Total number of loreal scales (LST): twenty-two (each side) (Williams character 11). Number of loreal scale rows (LSR): four (each side) (Williams character 10). Number of scale rows between suboculars and supralabials (SO/SPL): zero; the suboculars and supralabials are in contact (Williams character 15); contact formula 4/4 (four suboculars in contact with four supralabials) on each sides, although the configuration differs between the sides. Relative size and condition of scales anterior and posterior, respectively, to ear opening: subequal in size. Number of ventral scales in one head length (ventrHL): approximately 60. Number of dorsal scales in one head length (dorsHL): approximately 70. Number of ventral scales between levels of axilla and groin (ventrAG): not counted because first, it seems redundant with the number of ventral scales in one head length and second, because it is difficult to count accurately for the reasons given by Kohler (2014) for counting the scales in one-half the head length. Number of dorsal scales between levels of axilla and groin (dorsAG): not counted because first, it seems redundant with the number of dorsal scales in one head length and second, because it is difficult to count accurately for the reasons given by Köhler for counting the scales in one-half the head length. Number of rows of enlarged dorsal scales (RED): two rows of slightly enlarged middorsal scales (they are less than 1.5 times as large as adjacent scales). Condition of dorsal scales (CDS): smooth, granular, non-overlapping (Williams character 20). Condition of lateral body scales (LBS): smooth, granular, non-

overlapping. Condition of ventral scales (CVS): smooth, subimbricate, with rounded posterior margins; arranged in more-or-less transverse rows. Size of dorsal, lateral, and ventral scales: dorsal scales ca. 0.2 mm long, lateral scales ca. 0.15 mm long, ventral scales ca. 0.25 mm long (i.e., measured anterior to posterior). Number of scales around midbody (SAM): not counted; the small size of the scales makes this character very difficult to count accurately. Condition of dorsal caudal scales (DCS): moderately enlarged relative to adjacent laterals, imbricate, unkeeled anteriorly but keeled posteriorly. Condition of lateral caudal scales (LCS): unkeeled, weakly imbricate, arranged in rows of 8 scales per caudal segment, decreasing to 7 and then to 6 posteriorly. Condition of ventral caudal scales (VCS): More than two times longer than smallest laterals of the same segment, smooth anteriorly but keeled and mucronate posteriorly, imbricate throughout. Condition of terminal phalanx (CTP). This character is better described as the condition of the adhesive pad (of pedal digit IV) relative to the antepenultimate phalanx. In USNM 5095, the pad extends distally beyond the joint between the antepenultimate and penultimate phalanges, thus underlapping the proximal subdigital scales of the penultimate phalanx (Williams character 27). Note that the terminal=ultimate=ungual phalanx is small and does not extend proximally much beyond the claw, so that the part of the digit distal to the pad is often erroneously considered to involve a single phalanx, rather than two phalanges, and thus this character is erroneously described as the condition of the terminal (rather than penultimate) phalanx. Condition of axillary region: an axillary depression but no tube-like axillary pocket. Dewlap size (DS): Dewlap size was not measured (which is difficult on a preserved specimen), but the dewlap is large. The second ceratobranchials (which support the dewlap ventrally) extend well beyond the level of the insertion of the forelimbs and probably beyond the posterior end of the xiphisternal rods. Dewlap scalation: gorgetals smooth, non-overlapping, arranged in single rows; marginal dewlap scales smooth, overlapping.

Coloration. The general color of the body in preservative is brownish grey with traces of bluish iridescence, suggesting a greenish coloration in life (green lizards are commonly blue or purple in preservative; Savage & Talbot 1978), especially in the temporal region. There are brown reticulations on the dorsal part of the neck and anterior trunk, as well as a few dark spots on the sides of the neck and in the shoulder region. There appears to be a broad, light stripe running from the axilla to the groin and a narrower, shorter one in the shoulder region. The snout is brownish and there are traces of a dark transverse bar at the level of the orbits. The ventral skin of the body is light and unmarked; that in the gular region has several brown spots. There are indications of dark bars on both forelimbs and hindlimbs, including the digits. There is also brown pigmentation in the dorsal part of the sacral region and the proximal dorsal part of the tail, as well as indications of dark barring on the tail posteriorly.

Skeletal Morphology (Figs. 3 and 4)

To facilitate comparisons, we will present descriptions of the standard skeletal characters described by Etheridge (1959) and by Poe (2004) separately despite the partial redundancy.

Characters of Etheridge (1959). Palatine teeth: USNM 5095 appears to lack palatine teeth, although the palatine appears rugose in the region where teeth are present in *Chamaeleolis*. The presence versus absence of pterygoid teeth could not be determined unequivocally from our CT images (there is a ridge in the area where pterygoid teeth are present in other anole species, but individual teeth could not be distinguished). Angular: No indication of an angular bone was observed in the CT images, although its absence could not be determined unambiguously given the small size of the bone when present in anoles. Parietal shape: The parietal is Y-shaped with a short posterior crest; the parietal extends posteriorly to partially but not completely obscure the supraoccipital in dorsal view ("half-funnel" of Etheridge 1959). Parietal foramen: The parietal foramen lies within the frontoparietal suture, with the larger portion of its border within the parietal. Splenial: The splenial bone appears to be absent. Jaw sculpturing: The ventral surface of the dentary is smooth; it does not exhibit any of the three types of sculpturing described by Etheridge. Pectoral girdle: The lateral processes of the interclavicle form angles of ca. 52 (left) and 54 (right) degrees relative to the posterior process; they are in contact with the clavicles for most of their lengths (this corresponds to the "T-shaped" interclavicle category of Etheridge 1959, which seemingly has more to do with the association between clavicles and interclavicle than the actual shape of the interclavicle). Caudal sequence (transverse processes): The caudal sequence conforms to the "first iguanid type" of Etheridge (1959)—that is, there is a short series of anterior caudal vertebrae each bearing a single pair of transverse processes, but the posterior vertebrae lack transverse processes; autotomy septa, if present, begin near the posterior end of the series of anterior caudal vertebrae that bear transverse processes. More specifically, in USNM 5095, caudal vertebrae 1–9 bear transverse processes, vertebrae 1–7 are aseptate, 8 may or may not have a septum, and 9 is fractured at the septum, which is located just anterior to

the small and last pair of transverse processes. All the remaining vertebrae (10–21) are septate, with fractures at the septa of vertebra 13 and 21, the latter of which continues as a cartilaginous rod that represents the regenerated part of the tail. Caudal autotomy: present (the tail has been fractured and regenerated). Number of presacral vertebrae: 24. Anterior aseptate caudal vertebrae: seven or eight. Lumbar vertebrae (posterior presacral vertebrae that lack ribs): four. Sternal and xiphisternal ribs: Five pairs of ribs (connected to vertebrae 9–13) have cartilaginous connections to the sternum and xiphisternum. Post-xiphisternal inscriptional ribs: There are three attached and one unattached pairs of such ribs.

FIGURE 3. Reconstructions of the skeleton of USNM 5095 from CT scans in dorsal (top), lateral (middle), and ventral (bottom) views. The tail is broken off at the fracture plane in caudal vertebra 9 and is broken and displaced at the fracture plane in caudal vertebra 13 but has been digitally restored to its condition prior to damage. Scale bar = 1 cm.

Characters of Poe (2004). 47. Modal postxiphisternal inscriptional rib formula: 3:1 (state 7). 48. Modal number of sternal ribs: three (state 1). USNM 5095 is scored as having three sternal ribs based on correspondence between

its morphology and those of anoles considered to have three sternal ribs by Etheridge (1959: Fig. 4c, d), although we did not see a gap between the calcifications of the sternum and xiphisternum as illustrated by him. The third pair attaches to the anterior rod-like part of the sternum-xiphisternum complex but is likely homologous with the third rib pair of species in which that pair attaches to the sternal plate (e.g., Etheridge 1959: Fig. 4b). 49. Caudal vertebrae: alpha type (state 0). See the description of the caudal sequence under the characters of Etheridge (1959) for a more detailed description (Etheridge's "first iguanid type" of caudal sequence is often termed the "alpha type" because it is characteristic of the group that he recognized as the alpha section of *Anolis*). 50. Interclavicle: T-shaped (state z). See the description of the pectoral girdle under the characters of Etheridge (1959) for a more detailed description (the "T-shaped" category has more to do with the association between the lateral processes of the interclavicle and the clavicles than the actual shape of the interclavicle). 51. Modal number of presacral vertebrae: 24 (state 0). 52. Modal number of lumbar vertebrae: four (state 1). Presacral vertebrae 21–24 lack ribs. 53. Modal number of caudal vertebrae anterior to first autotomic vertebra: eight (state 3) or seven (state 4). Caudal vertebra number 7 lacks septa; caudal vertebra number 8 may or may not have them; caudal vertebra number 9 is fractured at the septum. 54. Caudal autotomy septa: present (state a). Autotomy septa are present in vertebrae 9–21 (number 21 is broken and bears a cartilaginous extension representing the regenerated part of the tail). 55. Supraoccipital cresting: lateral processes distinct from supraoccipital crest (state 1). The lateral processes of supraoccipital are separated from the medial process (the *processus ascendens tectum synoticum*). 56. Dorsal surface of skull: intermediate (state n), used for species with pronounced wrinkling but lacking pustulate tubercles. In USNM 5095, rugosities are present, especially on frontal and prefrontal bones, where they take the form of wrinkles rather than tubercles. 57. Parietal crests: form a Y without a spur (state 2). The parietal crests form a Y, with the posterior leg less then one-half the length of the lateral crests (length posterior crest/length lateral crest = ca. 0.37). 58. Anterolateral corners of parietal crests: reach posterolateral corners of frontal (state a). 59. Parietal casque: absent (state a). The parietal roof does not extend posterolaterally over the supratemporal processes. 60. Pineal foramen at parietal/frontal suture (state a). The foramen is located within the fronto-parietal suture with a larger portion in the parietal than the frontal. 61. Supratemporal processes (of parietal): extend over supraoccipital (state z). The *processus ascendens tectum synoticum* is not visible in dorsal view. 62. Postfrontal: present (state a). 63. Prefrontal: separated from nasal by frontal and maxilla (state z). The scoring of this character is not completely unambiguous from our CT images, but it appears that prefontal-nasal contact is absent and maxilla-frontal contact is present. 64. Frontal: sutures only with nasals anteriorly (state 0). There is no unossified gap between the frontal and nasals, although there is a small hole on each side; the premaxilla does not appear to contact the frontal. 65. Parallel crests extending longitudinally down nasals from frontal to nares: present (state z). The crests are present (bordering the prefrontal depression), but they are less parallel than in *A. carolinensis*, converging anteriorly. 66. Anterior edge of nasal: forms posterior border of naris (state a). In *A. equestris*, which is scored state z by Poe (2004), the nasal is excluded from the border of the naris by contact between the maxilla and premaxilla; USNM 5095 does not exhibit that condition. 67. Dorsal process of jugal: terminates on posterior aspect of postorbital (state a). 68. Contact between jugal and squamosal: absent (state a). 69. Posteroventral corner of jugal: is anterior to posterior edge of jugal (state a). 70. Epipterygoid: contacts parietal (state a). 71. Pterygoid teeth: There is a ridge on the pterygoid where pterygoid teeth are located in other anoles, but the presence versus absence of pterygoid teeth could not be determined from our CT images. 72. Lateral edges of vomer: smooth (state a). The lateral edges of the vomers are more or less straight and lack posteriorly directed lateral processes. 73. Maxilla: extends posteriorly to ectopterygoid (state a). The maxilla does not extend posterior to the posterior terminus of the lateral process of the ectopterygoid. 74. Basipterygoid crest: absent (state a). There are no anteroventral crests on the basipterygoid processes. 75. Quadrate lateral shelf: present (state z). 76. Black pigment on skull: This character could not be scored because we scored osteological characters from CT images rather than dry skeletons. 77. Premaxilla (relationship to nasals): The sutures between nasals and premaxilla could not be seen well enough to score this character. 78. Posterior of skull: slopes inferiorly (state z). The skull in this region slopes slightly inferiorly. 79. Crenulation along lateral edges of parietal: absent (state a). 80. Parietal roof: flat (state a). The parietal roof is scored as flat, but it is actually somewhat concave, as there is a parietal depression; it is not convex. 81. Posteriormost tooth: is at least partially anterior to anterior mylohyoid foramen (state m). On both right and left sides, the posteriormost dentary tooth is situated partially anterior to the anterior edge of the anterior mylohyoid foramen. 82. Angular process of articular: present, large (state a). 83. Posterior suture of dentary: blunt (state z?). The lateral dentary-surangular suture is not entirely clear in our CT images, but it does not appear to be pronged. 84. Anteriormost aspect of posterior border of dentary: within mandibular fossa (state z). 85. Splenial:

absent (state 2). The splenial appears to be absent, although presence as a sliver cannot be ruled out based on our CT images. 86. Anteromedial process of coronoid: extends anteriorly (state a). The posterior edge of the anteromedial process of the coronoid lacks a posteriorly projecting process. 87. Surangular foramen: completely in surangular (state a). 88. Coronoid labial process: present (state z). 89. Posterolateral aspect of coronoid: extends into or beyond supra-angular foramen (state z). The posterolateral process of the coronoid extends roughly to the level of the supra-angular foramen. 90. Jaw sculpturing in large adult males: absent (state 0). 91. Angular bone: absent (state z?). The angular bone appears to be absent, but this cannot be determined with certainty from our CT images.
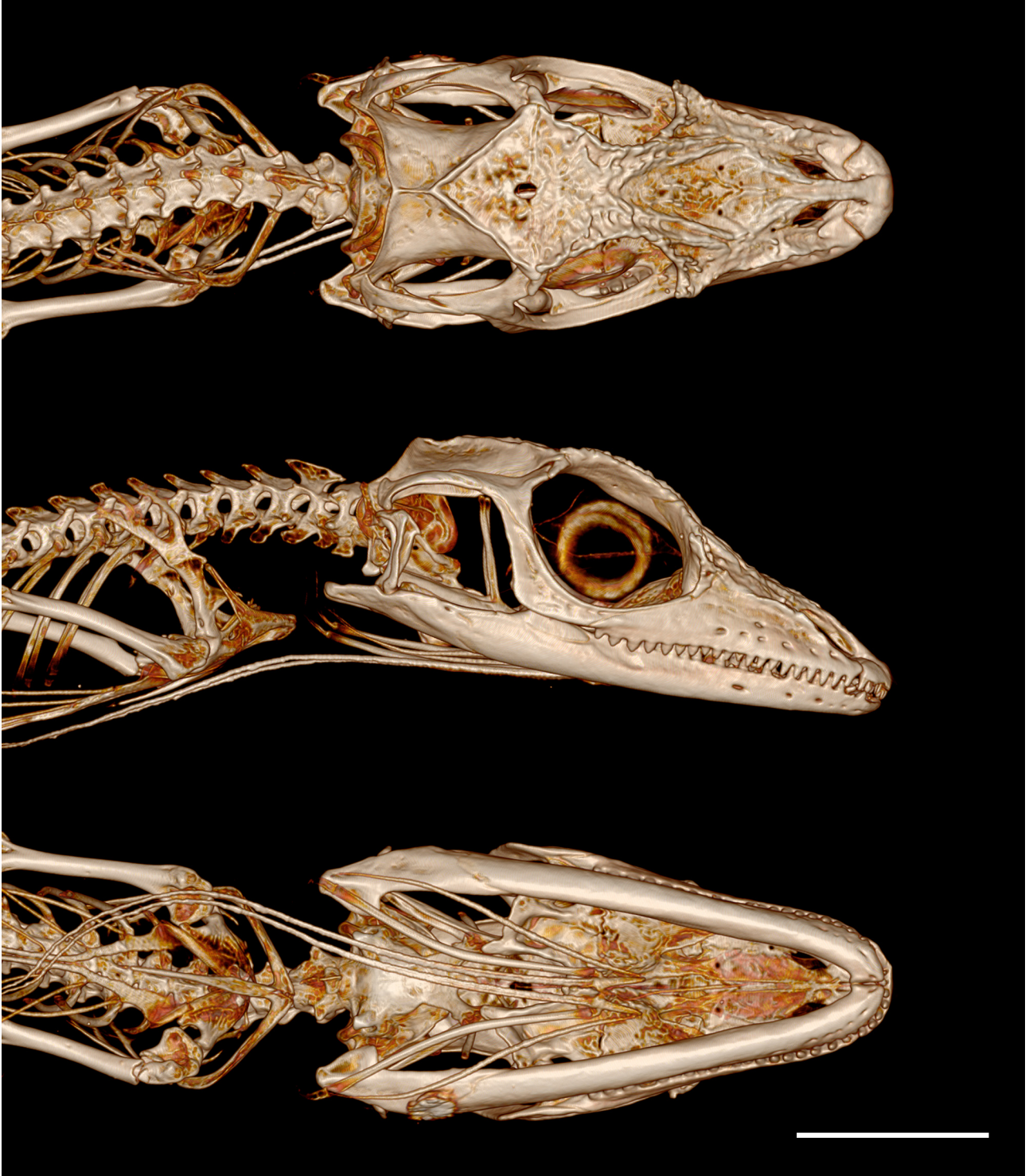

FIGURE 4. Reconstructions of the skeleton of the head and anterior body of USNM 5095 from CT scans in dorsal (top), lateral (middle), and ventral (bottom) views. Scale bar = 5 mm.

Comparisons

With the Type of *A. incredulus*

We compared USNM 5095 with the description provided by Garrido & Moreno (1998) for the holotype of *Anolis incredulus* (CZACC 4.7394). The comparisons involve 26 characters and are summarized in Table 1. The two specimens agree exactly or nearly so for 18 of the characters (1, 2, 3, 4, 5, 6, 7, 8, 9, 11, 12, 14, 16, 19, 20, 24, 25, 26), including (most importantly) those that describe the general size and arrangement of the head scales, the relative sizes and texture of the body scales, and the coloration. Five of the characters involving counts and one involving a ratio differ slightly (characters 13, 15, 17, 18, 22, 23) but are within the range of variation observed in other anole species. The two specimens differ markedly in dewlap size (character 10): that of the holotype having been described as vestigial while that of USNM 5095 is large. Given that the holotype is a female and USNM 5095 is a male, this difference likely reflects sexual dimorphism in dewlap size, which is common among *Anolis* species (Harrison & Poe 2012). Finally, the two specimens differ in the number of ventral scales in a distance corresponding to the snout length (character 21). This difference is difficult to evaluate without detailed knowledge of allometric growth and sexual dimorphism, but it could be the result of males having relatively longer snouts, which is common among *Anolis* species (Sanger *et al.* 2013).

With Members of the *Anolis isolepis* Species Group (Figs. 5, 6, and 7)

We will use the informal name "*Anolis isolepis* species group" for a clade including *A. isolepis* and its closest relatives. This group is currently thought to include five extant species (phylogenies of Poe *et al.* 2017; Díaz *et al.* 2022): *A. isolepis* Cope 1861, *A. altitudinalis* Garrido 1985, *A. toldo* Fong & Garrido 2000, *A. oporinus* Garrido & Hedges 2001, and *A. viridulus* Díaz *et al.* 2022. As the members of this group are highly similar, we will emphasize comparisons with the species that occur in the Sierra Maestra: *A. isolepis*, *A. altitudinalis*, and *A. oporinus*. In addition to the specimens that we examined for these comparisons, data were also obtained from Barbour & Ramsden (1919), Ruibal (1964), Garrido (1985), Garrido & Hedges (2001), and Díaz *et al.* (2022).

USNM 5095 differs from members of the *Anolis isolepis* species group in many respects, including the following: Its dorsal head scales are smooth or rugose, whereas members of the *A. isolepis* species group have striated dorsal head scales. It has a narrow rostral scale (< 1/2 the width of the mental scales) compared to a wide rostral scale (> 1/2 the width of the mental scales, measured along the curve of the lip). Related to the previous character, it has four postrostrals versus five or more postrostrals. It has 10 scales between the second canthals versus four–five such scales and rarely as many as seven. It has well developed frontal ridges and a distinct frontal depression versus very weakly developed frontal ridges and almost no frontal depression so that the surface of the head in the frontal region is nearly flat. It has two distinctly enlarged supraoculars (each side) that are surrounded by much smaller scales versus three or (usually) more moderately enlarged supraoculars that exhibit more or less continuous gradation in size with the other supraoculars. It has the enlarged supraoculars separated from the supraorbitals by two rows of smaller scales versus the enlarged supraoculars either in contact with the supraorbitals or separated from them by one row of smaller scales. In USNM 5095, the interparietal is large and contacts the supraorbital semicircles at its anterolateral corners versus small and usually separated from the supraorbital semicircles by one or more scales. It has 22 loreals in four rows versus 17 or fewer loreals in two–three rows. It has one sublabial (each side) in contact with the infralabials versus two or more sublabials in contact with the infralabials. It lacks enlarged postcloacal scales versus enlarged postcloacal scales present in males. It has a distinctly compressed tail versus a cylindrical to weakly compressed tail.

With Members of the *Anolis angusticeps* Species Group (Figs. 5, 6, and 7)

We will use the informal name "*Anolis angusticeps* species group" for a clade including *A. angusticeps* and its closest relatives. This group is currently thought to include four to eight extant species (phylogenies of Poe *et al.* 2017; Nicholson *et al.* 2012): *A. angusticeps* Hallowell 1856, *A. paternus* Hardy 1967, *A. oligaspis* Cope 1894, *A. alayoni* Estrada & Hedges 1995, and possibly *A. sheplani* Schwartz 1974, *A. placidus* Hedges & Thomas 1989, *A. guazuma* Garrido 1983, and *A. garridoi* Díaz, Estrada & Moreno 1996. Although *A. guazuma* is not strongly supported as a member of this clade, for the sake of convenience, we will treat it as though it is. Again, we will emphasize comparisons with species that occur in the Sierra Maestra: *A. angusticeps* and *A. guazuma*. In addition to the specimens that we examined for these comparisons, data were also obtained from Barbour & Ramsden (1919), Ruibal (1964), Garrido (1983), and Estrada & Hedges (1995).

TABLE 1. Comparison of the holotype of *Anolis incredulus* (CZACC 4.7394) with USNM 5095 based on the characters described for the holotype by Garrido and Moreno (1998). L = left side, R= right side.

|	Character	Holotype	USNM 5095
1	Head length/head width	1.9	1.9
2	Dorsal head scales and gular scales	Smooth	Smooth (some rugose)
3	Interparietal	Large and rugose	Large and rugose
4	Parietal eye	Small	Small
5	Scales surrounding interparietal	Large	Large
6	Interparietal/supraorbital semicircles	In contact (L), almost in contact (R)	In contact or almost in contact at anterolateral corners
7	Nuchal scales	Gradually decreasing in size posteriorly	Gradually decreasing in size posteriorly
8	Parietal scales	Smaller than those that surround the interparietal and larger than the dorsals	Smaller than those that surround the interparietal and larger than the dorsals
9	Infraorbitals	In contact with supralabials	In contact with supralabials
10	Dewlap	Vestigial	Large
11	Supraorbital semicircles	Separated by one row of scales	Separated by one row of scales
12	Enlarged supraoculars	Three on one side, two on the other	Two on each side
13	Loreals	Some 23	22 (each side)
14	Scales between (first) canthals	Seven	Seven
15	Scales bordering rostral	Seven	Six
16	Postmentals	Six	Six
17	Supralabials	Eight	Nine
18	Infralabials	Eight	Nine
19	Dorsal Scales of Body	Very small, smooth, uniform	Very small, smooth, uniform
20	Ventral Scales of Body	Smooth and slightly larger than dorsals	Smooth and slightly larger than dorsals
21	Number of ventrals in the snout length	19	27
22	Subdigital lamellae on pedal digit IV	17	20
23	Snout-vent length/femur length	4.5	5.2
24	Coloration in Life	Green (stated by authors)	Green (inferred)
25	Coloration in alcohol	Grayish-leaden with semi-oval whitish shoulder mark	Brownish grey with blue iridescence and a light shoulder stripe
26	Coloration of lower leg and toes	Carmel color (contrasting with the color of the thigh and the rest of the body)	Brown bars
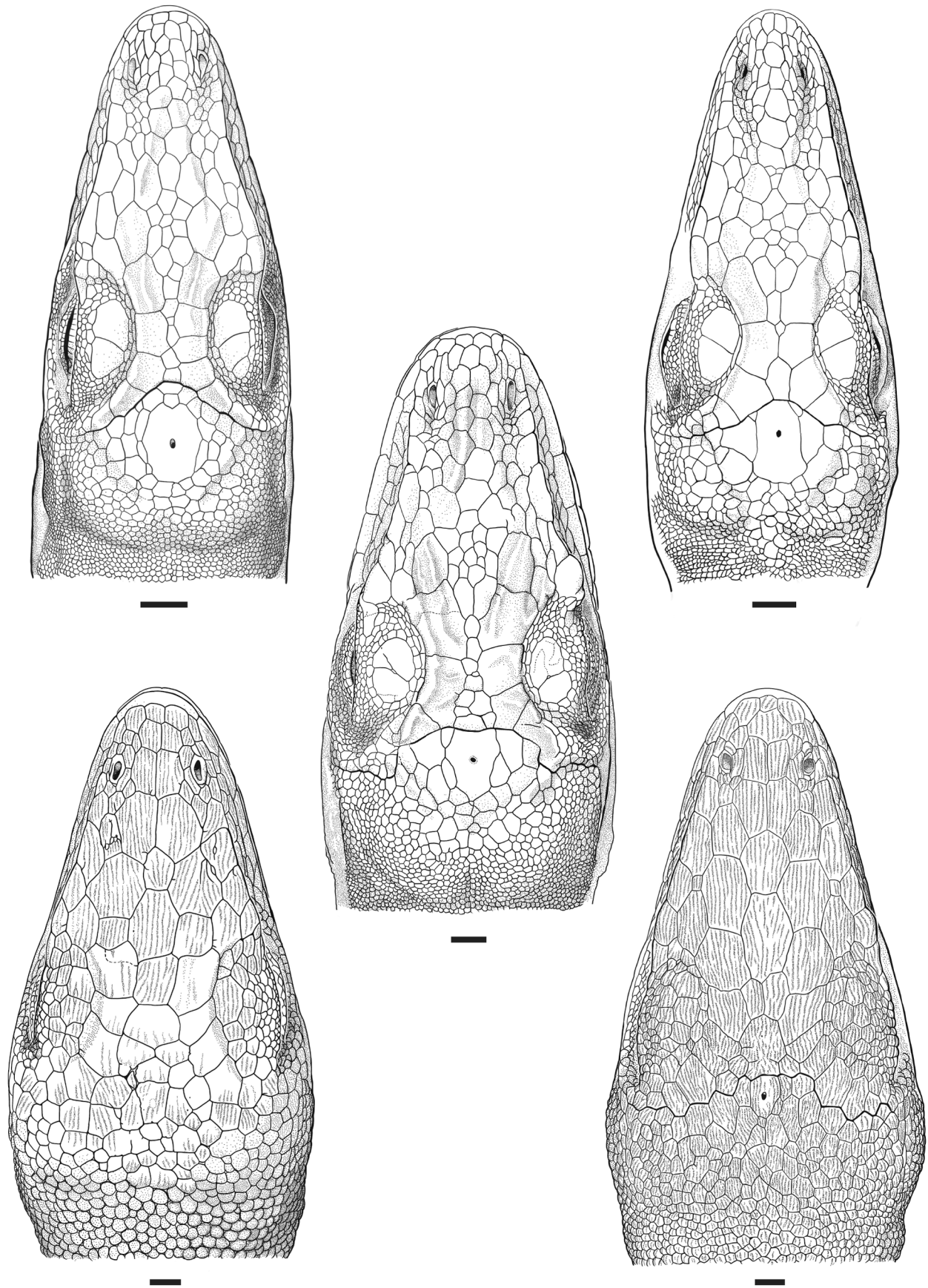
FIGURE 5. Line drawings of the head scales of *Anolis incredulus* (USNM 5095; middle) in dorsal view compared with those of *A. angusticeps* (USNM 497990; upper left), *A. guazuma* (USNM 589689; upper right), *A. altitudinalis* (USNM 538874; lower left), and *A. isolepis* (USNM 589701; lower right). Scale bar = 1 mm.
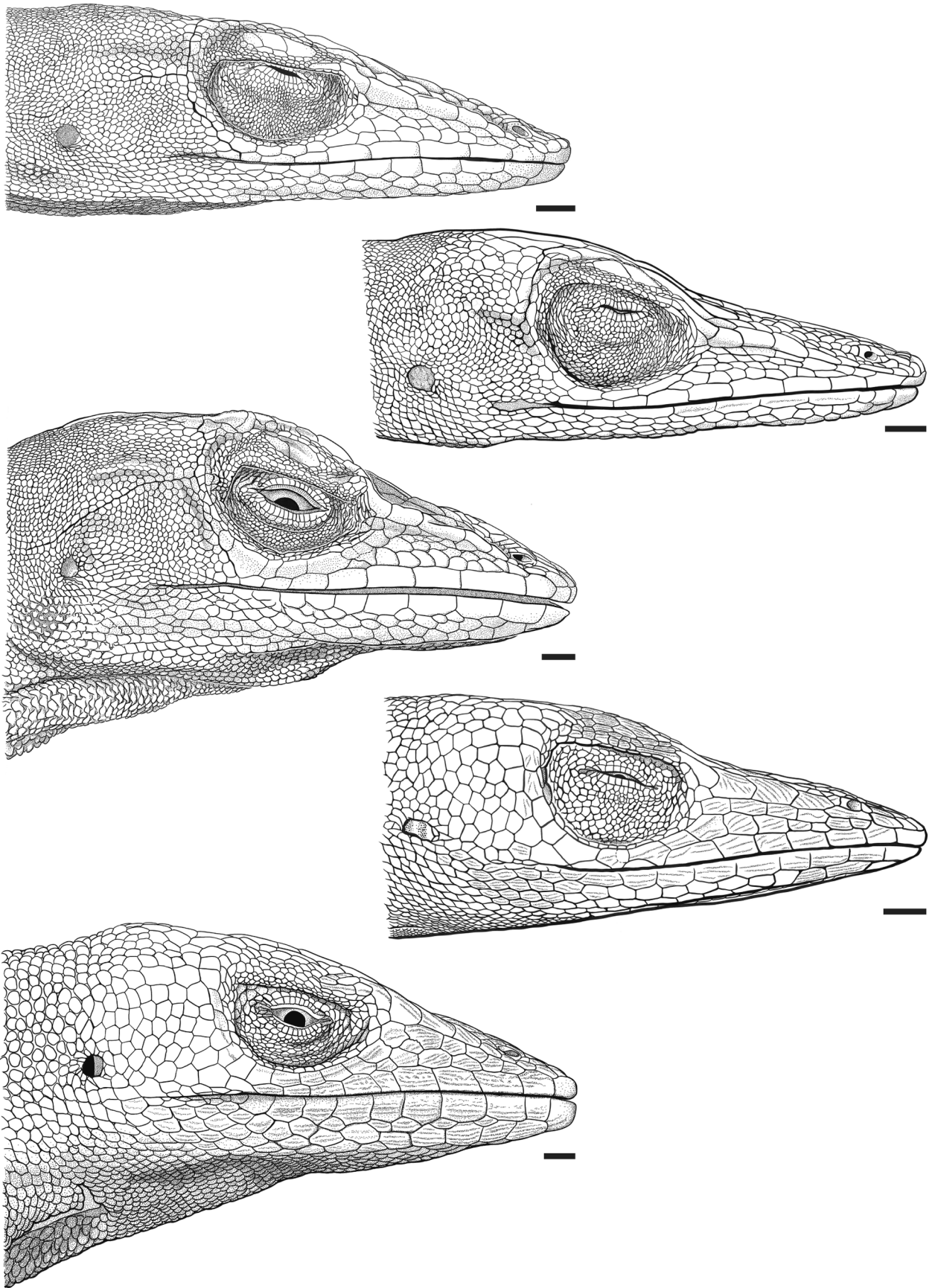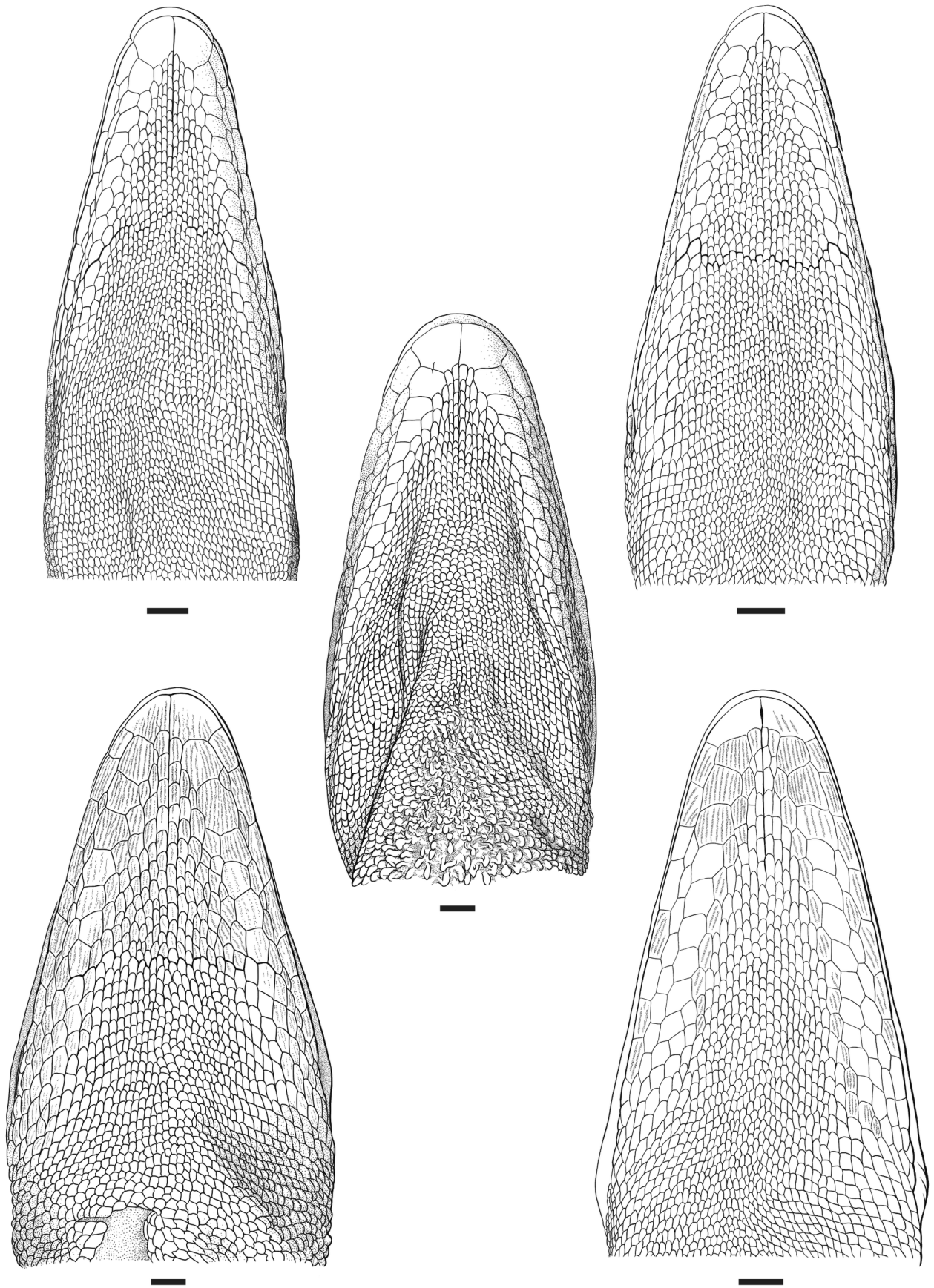
FIGURE 6. Line drawings of the head scales of *Anolis incredulus* (USNM 5095; middle) in lateral view compared with those of *A. angusticeps* (USNM 497990; upper left), *A. guazuma* (USNM 589689; upper right), *A. altitudinalis* (USNM 538874; lower left), and *A. isolepis* (USNM 589700; lower right). Scale bar = 1 mm.

FIGURE 7. Line drawings of the head scales of *Anolis incredulus* (USNM 5095; middle) in ventral view compared with those of *A. angusticeps* (USNM 497990; upper left), *A. guazuma* (USNM 589689; upper right), *A. altitudinalis* (USNM 538874; lower left), and *A. isolepis* (USNM 589700; lower right). Scale bar = 1 mm.

Although USNM 5095 is arguably more similar to members of the *Anolis angusticeps* species group than to those of the *Anolis isolepis* species group, it still differs from the former in several respects, including the following: Although similar to *A. angusticeps* and *A. guazuma* in SVL (maxima of all species in the 45–50 mm range), USNM 5095 is distinctly larger because it is more thickly built. It also has a broader head and, presumably related to this, more scales between canthals (10 versus modes of 7). The frontal ridges and frontal depression are more strongly developed. Its rostral scale is narrower and, presumably related to this, it has fewer postrostrals (4 versus 6–8). It lacks enlarged postcloacal scales versus enlarged postcloacal scales present in males. It has a distinctly compressed tail versus tails that are nearly round in cross section. It is thought to have been greenish in life versus gray or brown. In addition, USNM 5095 is similar to most specimens of *A. guazuma* in having contact between the interparietal and supraorbital semicircles whereas the usual condition in *A. angusticeps* is the absence of contact. Finally, USNM 5095 has a 3:1 postxiphisternal inscriptional rib formula versus 3:2 in the one specimen of *A. guazuma* examined (USNM 589689) while *A. angusticeps* is reported to have a modal condition of 2:2 (Etheridge 1959; Poe 2004).

With *Anolis porcatus*

In some respects, particularly its inferred green coloration and well developed canthal and frontal ridges, *Anolis incredulus* (USNM 5095) gives the impression of a dwarf *Anolis porcatus*, the widespread species of trunk crown anoles in Cuba. Moreover, as mentioned above (see The Specimen), USNM 5095 was originally catalogued as part of a lot of 7 specimens, all remaining members of which are now identified as *A. porcatus*. However, in addition to its smaller size, *A. incredulus* differs from *A. porcatus* in many respects, including having a shorter snout, an inferred shorter tail, an only slightly enlarged superciliary scale, fewer and more distinctly enlarged supraocular scales, contact between the interparietal and supraorbital semicircles, lack of keeling on the dorsal and ventral body scales, and fewer fourth toe lamellae.

Inferences from the Comparisons.

Based on the above comparisons, which constitute differential diagnoses, USNM 5095 differs in several important ways from members of both the *Anolis isolepis* and the *Anolis angusticeps* species groups (as well as *A. porcatus*). It therefore seems highly unlikely that it belongs to any of the currently known species in either of those groups. By contrast, USNM 5095 exhibits close agreement with the holotype of *Anolis incredulus*, particularly regarding the general size and arrangement of the head scales, the relative sizes and texture of the body scales, and the coloration. Most of the differences between the two specimens are within the range of variation seen in other anole species or are attributable to sexual dimorphism. Lacking any clear evidence that the two specimens are from different species, we consider it parsimonious to treat them as conspecific. Of course, it is possible that they are not truly conspecific, but even if they are not, they would seem to be members of highly similar and presumably closely related species.

Phylogenetic relationships

The scores of USNM 5095 for the 46 morphological characters used by Poe *et al.* (2017) are as follows: 1: 0, 2: 2, 3: {0,1}, 4: 4, 5: 0, 6: 0, 7: ?, 8: 4, 9: 5, 10: 1, 11: 0, 12: {2,3,4,5}, 13: 5, 14: 0, 15: 2, 16: 3, 17: 0, 18: 1, 19: 1, 20: 1, 21: 5, 22: 0, 23: 5, 24: 0, 25: 2, 26: 0, 27: 0, 28: 0, 29: 0, 30: 2, 31: 5, 32: 5, 33: 0, 34: 0, 35: 0, 36: 0, 37: 0, 38: 0, 39: 0, 40: 5, 41: 0, 42: 1, 43: 1, 44: ?, 45: ?, 46: ?. (We note that characters 11, 12, and 31 are incorrectly described in Appendix 2 of Poe *et al.* (2017) as three-state characters but are correctly scored in the data file as six-state characters.) We performed the phylogenetic analysis using the *Ctenocercus* clade (Poe *et al.* 2017), with the addition of *A. incredulus*, as the ingroup and *A. cristatellus* as the outgroup (Poe *et al.* 2017). *A. incredulus* is inferred to belong to the *Ctenocercus* clade based on its "half-funnel" parietal morphology (all species in the group), absence of a splenial bone (all species in the group except *A. longiceps* (Etheridge 1959)), "T-shaped" clavicle-interclavicle morphology (all species in the group), 3:1 inscriptional rib formula (other species 3:1 or 2:2), "alpha" type of caudal vertebrae (all species in the group), and Cuban distribution (all species except *A. sheplani* and *A. placidus*, which are inferred to have colonized Hispaniola from Cuba (Poe *et al.* 2017), and various close relatives of *A. porcatus*, which are inferred to have colonized the Bahamas, the Cayman Islands, Navassa Island, and the North American mainland from Cuba (Glor *et al.* 2005)). The *Ctenocercus* clade is an ancestrally and predominantly Cuban radiation that includes all of the Cuban *Anolis* species except the giant twig anoles of the *Chamaeleolis* clade, the giant crown

anoles of the *Anolis equestris* complex, the dewlapless and ecologically distinctive *A. bartschi* and *A. vermiculatus*, and the trunk-ground and grass anoles of the *Trachypilus* clade (Poe *et al.* 2017). Moreover, the *Ctenocercus* clade includes all the species that have been considered potential close relatives of *A. incredulus*—that is, members of the *A. isolepis* species group and the *A. angusticeps* species group (including *A. guazuma*).
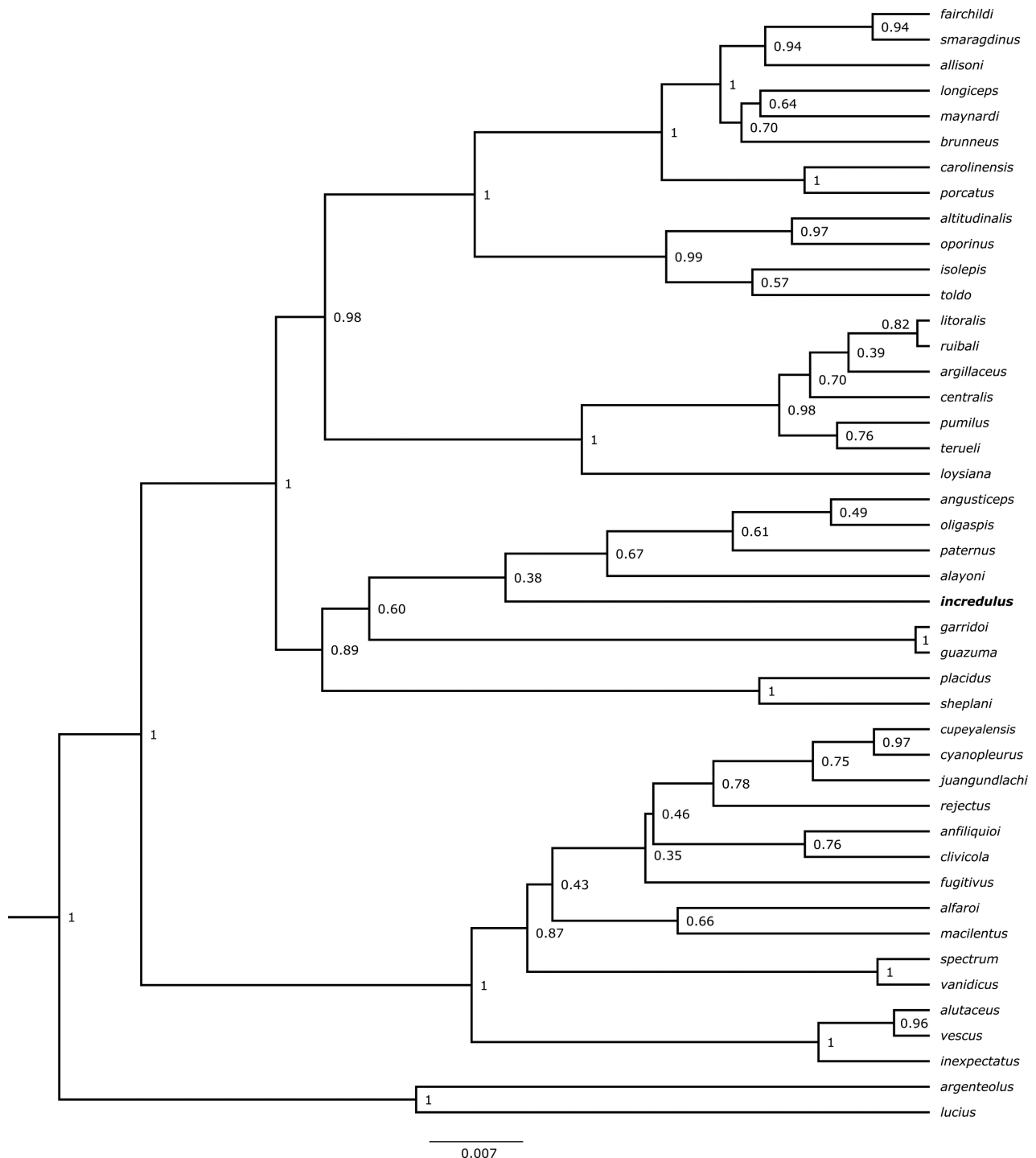

FIGURE 8. Phylogenetic relationships of *A. incredulus* (bold text) estimated from its scores for 46 morphological characters integrated into the dataset of Poe *et al.* (2017) and analyzed using Bayesian phylogenetic inference under an uncalibrated relaxed clock with the *Ctenocercus* clade (all species shown) as the ingroup and *A. cristatellus* (not shown) as the outgroup. Numbers adjacent to nodes are Bayesian posterior probabilities (PP). *A. incredulus* is inferred to be nested within two large clades within *Ctenocercus* with strong support (PP = 1.00) and within a clade of twig anoles (*A. angusticeps* through *A. sheplani*) with moderate support (PP = 0.89). Its exclusion from each of the three largest clades within *Ctenocercus* that are non-overlapping relative to the twig anole clade, as well as from the two main subclades of the largest of those clades, is also strongly supported (PP = 0.98–1.00). Scale bar indicates the average number of substitutions per site.

The Bayesian phylogenetic analysis is inferred to have reached convergence based on an average standard deviation of split frequencies <0.01 (final value = 0.005133), no trend to increase or decrease in log probabilities for the post burn-in samples as well as extensive overlap in the log probabilities between the two runs, all effective sample sizes of parameters >100 (for both average and minimum ESS), and all potential scale reduction factor values for parameters very close to 1.00 (greatest departure = 1.002). The results of our phylogenetic analysis (Fig. 8) indicate that *A. incredulus* in nested deep within the *Ctenocercus* clade, in strongly supported clades that include 1) all *Ctenocercus* species except *A. argenteolus* and *A. lucius* (posterior probability, PP = 1.00), 2) a subclade of twig anoles related to *A. angusticeps* plus a subclade of mostly trunk-crown anoles related to *A. carolinensis* plus a subclade of species mostly unassigned to ecomorph (Losos 2009) related to *A. loysiana* (although *A. loysiana* is classified as a trunk anole) (PP = 1.00). *A. incredulus* is also placed in the twig anole clade, which is moderately supported (PP = 0.89), and there is strong support for it not being included in the clades of mostly trunk-crown anoles related to *A. carolinensis* (including the *A. isolepis* species group as recognized in the previous section) and of species mostly unassigned to ecomorph related to *A. loysiana* (PP = 1.00 for both) or in the larger clade composed of those two subclades (PP = 0.98). The relationships of *A. incredulus* within the clade of twig anoles are not well supported.

Our results corroborate the hypothesis of Garrido & Hedges (2001), who suggested that *A. incredulus* was not a member of what we have called the *A. isolepis* species group, and that of Díaz *et al.* (2022: 13), who stated that "all the external characters of this specimen [the holotype of *A. incredulus*] show that it is a twig anole related to *Anolis angusticeps*" and therefore that it is not a member of what they recognized as the *carolinensis* species group, including the *isolepis* subgroup. However, because the inferred phylogenetic position of *A. incredulus* is currently based solely on morphological characters and its exact relationships are not well supported, it will be important to collect additional specimens of this species to test those relationships with DNA sequence data.

The results of our phylogenetic analysis are largely congruent with those of Poe *et al.* (2017), with some minor differences among nodes that are not strongly supported in either tree, mostly in the clade of grass-bush anoles (*A. cupeyalensis* through *A. inexpectatus*). Perhaps the most important difference concerns the placement of the clade composed of *A. garridoi* and *A. guazuma*, which was weakly supported (PP = 0.53) as sister to the clade of species mostly unassigned to ecomorph(s) related to *A. loysiana* in the results of Poe *et al.* (2017) but is more strongly supported (PP = 0.89) as part of the twig anole clade in our results.

Ecological morphology

Our ecomorphological analyses (Table 2) assigned *Anolis incredulus* as well as *A. guazuma*, *A. isolepis*, and *A. altitudinalis* to the twig ecomorph category based on Linear Discriminant Analysis (LDA) and three Euclidean distance criteria (Huie *et al.* 2021). Similar results were obtained for the other three species when tail length (which was lacking for *A. incredulus*) was included (results not shown) and when standard (non-phylogenetic) PCA was used to calculate the Euclidean distances (except that *A. altitudinalis* was not assigned to any ecomorph based on the centroid distance criterion with tail length excluded; results not shown). In the case of *A. guazuma*, the twig ecomorph assignment was expected based on what is known of its natural history (Garrido 1983; Rodriguez Schettino 1999). In the case of *A. isolepis* and *A. altitudinalis*, the assignment seems incorrect, although the same assignment has been made for *A. isolepis* in previous analyses (Schaad & Poe 2010; Huie *et al.* 2021; see also Rand & Williams in Rodríguez Schettino *et al.* 2010). For a long time, little was known about the natural history of *A. isolepis* and its close relatives (Barbour & Ramsden 1919; Ruibal 1964). In June 1999, one of us (KdQ) had the opportunity to observe several *Anolis isolepis* individuals from an elevated platform in the vicinity of La Gran Piedra (Santiago de Cuba Province). The lizards were active on the surface of leaves in the crowns of small trees, as was previously reported by Losos (2009:53; see also Williams 1969). Díaz *et al.* (2022) reported that lizards of the closely related species *A. viridulus* were collected while roosting at night on leaves, and Losos (2009) classified all four of the then-known species in what we have called the *A. isolepis* species group as trunk-crown anoles. All species in this group are green, as is usual for trunk-crown anoles but not for twig anoles (Williams 1983; Losos 2009). It thus appears that the species in the *A. isolepis* species group may be trunk-crown anoles that are atypical in being more strongly specialized for living on leaves than are other members of the trunk-crown ecomorph. If such specialization is manifested in shorter limbs and tails and smaller body size, this could result in the lizards being misclassified as twig anoles.

TABLE 2. Results of the ecomorphological analysis using phylogenetic Principal Components Analysis and excluding tail length (because the tail of USNM 5095 is regenerated). Tw = Twig; LDA = Linear Discriminant Analysis (Discriminant Function Analysis) posterior probability for the predicted ecomorph assignment; CD = Centroid distance (given only if the Euclidean distance from the assessed species to the centroid of the predicted ecomorph is ≤ the distance of the furthest predetermined member of that ecomorph to the centroid); MPD = Mean pairwise distance (given only if the average Euclidean distance of the assessed species to all members of the predicted ecomorph is ≤ the largest average distance among the predetermined members of that ecomorph); NND = Nearest neighbor distance (given only if the distance of the assessed species to the nearest member of the predicted ecomorph is ≤ the largest nearest neighbor distance among the predetermined members of that ecomorph). All four species satisfied each of the three Euclidean distance criteria only for the twig ecomorph.

Species	Predicted Ecomorph	LDA	CD	MPD	NND
A. incredulus	Tw	1.000	0.188	0.460	0.272
A. altitudinalis	Tw	0.992	0.640	0.736	0.349
A. guazuma	Tw	1.000	0.210	0.439	0.165
A. isolepis	Tw	1.000	0.404	0.528	0.185

The twig ecomorph assignment of *A. incredulus* is difficult to evaluate, because almost nothing is known about the ecology of this species. The reported (holotype) and inferred (USNM 5095) green coloration of the two specimens suggests a trunk-crown species, and *A. incredulus* was classified as a trunk-crown species by Losos (2009). However, that assignment is contradicted by both our quantitative analysis of the morphology of USNM 5095 and the phylogenetic placement of *A. incredulus* within a clade of twig anole species. These seeming contradictions could be the result of structural habitat use that is consistent with assignment to a particular ecomorph but differs from that of other members of that ecomorph. For example, *A. incredulus* lizards could be trunk-crown anoles that make greater use of leaves than do the members of most other trunk-crown species, as we have suggested for *A. isolepis* and its close relatives, or they could be twig anoles that perch more commonly on green twigs than do the member of most other twig anole species (which tend to be gray rather than green, although greenish coloration occurs in some other twig anoles, such as Hispaniolan *Anolis insolitus*; Williams & Rand 1969). In any case, the appropriate ecomorph assignment for *A. incredulus* can only be determined by finding more specimens of this species and recording information on their structural habitat use.

Other considerations

Because of the poor condition of the holotype of *Anolis incredulus*, which was the basis for the recent proposal to consider the species a *species inquirenda* (Díaz *et al.* 2022), it might be tempting to petition the ICZN to designate USNM 5095 the neotype for that species under Article 75.5 (replacement of an unidentifiable name-bearing type). We have chosen not to do so for two main reasons. First, the description of the holotype (Garrido & Moreno 1998) is sufficient to distinguish *A. incredulus* from other currently known anole species and to refer specimens to that species, as we have done with USNM 5095. Second, although USNM 5095 seems to be in better condition than the holotype, it is also a damaged specimen and lacks precise locality data. Therefore, this specimen would not be very useful for determining the correct application of names were it to be made the name-bearing type for the species.

Acknowledgments

References

Barbour, T. & Ramsden, C.T. (1919) The herpetology of Cuba. *Memoirs of the Museum of Comparative Zoology at Harvard College*, 47 (2), 69–213, 15 pls.
https://doi.org/10.5962/bhl.title.49191

Díaz, L.M., Cádiz, A., Velazco, K. & Kawata, M. (2022) A new dwarf green anole (Squamata: Dactyloidae) of the *Anolis carolinensis* species group, from western Cuba. *Caribbean Herpetology*, 84, 1–16.
https://doi.org/10.31611/ch.84

Estrada, A.R. & Hedges, S.B. (1995) A new species of *Anolis* (Sauria: Iguanidae) from eastern Cuba. *Caribbean Journal of Science*, 31 (1–2), 65–72.

Etheridge, R. (1959) *The Relationships of the Anoles (Reptilia, Sauria, Iguanidae) an Interpretation based on Skeletal Morphology*. Ph.D. dissertation. University of Michigan, Ann Arbor, Michigan, 236 pp.

Feiner, N., Jackson, I.S.C., Munch, K.L., Radersma, R. & Uller, T. (2020) Plasticity and evolutionary convergence in the locomotor skeleton of Greater Antillean *Anolis* lizards. *eLife*, 9, e57468.
https://doi.org/10.7554/eLife.57468

Feiner, N., Jackson, I.S.C., Stanley, E. & Uller, T. (2021a) Evolution of the locomotor skeleton in *Anolis* lizards reflects the interplay between ecological opportunity and phylogenetic inertia. *Nature Communications*, 12, 1525.
https://doi.org/10.1038/s41467-021-21757-5

Feiner, N., Jackson, I.S.C., Van der Cruyssen, E. & Uller, T. (2021b) A highly conserved ontogenetic limb allometry and its evolutionary significance in the adaptive radiation of *Anolis* lizards. *Proceedings of the Royal Society of London B*, 288, 20210226.
https://doi.org/10.1098/rspb.2021.0226

Garrido, O.H. (1983) Nueva especie de *Anolis* (Lacertilia: Iguanidae) de la Sierra del Turquino, Cuba. *Caribbean Journal of Science*, 19 (3–4), 71–76.

Garrido, O.H. (1985) Nueva subespecie de *Anolis isolepis* (Lacertilia: Iguanidae) para Cuba. *Doñana, Acta Vertebrata*, 12 (1), 41–49.

Garrido, O.H. & Moreno, L.V. (1998) Nueva especie de *Anolis* (Lacertilia: Iguanidae) del Pico Turquino, Sierra Maestra, Cuba. *Avicennia*, 8/9, 35–40.

Garrido, O.H. & Hedges, S.B. (2001) A new anole from the northern slope of the Sierra Maestra in eastern Cuba (Squamata: Iguanidae). *Journal of Herpetology*, 35 (3), 378–383.
https://doi.org/10.2307/1565955

Glor, R.E, Losos, J.B. & Larson, A. (2005) Out of Cuba: overwater dispersal and speciation among lizards in the *Anolis carolinensis* subgroup. *Molecular Ecology*, 14 (8), 2419–2432.
https://doi.org/10.1111/j.1365-294X.2005.02550.x.

Harrison, A. & Poe, S. (2012) Evolution of an ornament, the dewlap, in females of the lizard genus *Anolis*. *Biological Journal of the Linnean Society*, 106 (1), 191–201.
https://doi.org/10.1111/j.1095-8312.2012.01847.x

Howard, R.A. (1988) *Charles Wright in Cuba, 1856–1867*. Chadwyck-Healey, Alexandria, Virginia, 90 pp.

Huie, J.M., Prates, I., Bell, R.C. & de Queiroz, K. (2021) Convergent patterns of adaptive radiation between island and mainland *Anolis* lizards. *Biological Journal of the Linnean Society*, 134, 85–110.
https://doi.org/10.1093/biolinnean/blab072

International Commission on Zoological Nomenclature (ICZN) (1999) *International Code of Zoological Nomenclature*. International Trust for Zoological Nomenclature, London, 306 pp.

Kikinis, R., Pieper, S.D. & Vosburgh, K.G. (2014) 3D Slicer: a platform for subject-specific image analysis, visualization, and clinical support. *In:* Jolesz, F.A. (Ed.), *Intraoperative Imaging and Image-guided Therapy*. Springer, New York, New York, pp. 277–289.

Köhler, G. (2014) Characters of external morphology used in *Anolis* taxonomy—Definition of terms, advice on usage, and illustrated examples. *Zootaxa*, 3774 (3), 201–257.
https://doi.org/10.11646/zootaxa.3774.3.1

Nicholson, K.E., Crother, B.I., Guyer, C. & Savage, J.M. (2012) It is time for a new classification of anoles (Squamata: Dactyloidae). *Zootaxa*, 3477 (1), 1–108.
https://doi.org/10.11646/zootaxa.3477.1.1

Losos, J.B. (2009) *Lizards in an Evolutionary Tree: Ecology and Adaptive Radiation of Anoles*. University of California Press, Berkeley, California, 507 pp.

Poe, S. (1998) Skull characters and the cladistic relationships of the Hispaniolan dwarf twig *Anolis*. *Herpetological Monographs*, 12, 192–236.
https://doi.org/10.2307/1467021

Poe, S. (2004) Phylogeny of anoles. *Herpetological Monographs*, 18, 37–89.
https://doi.org/10.1655/0733-1347(2004)018[0037:POA]2.0.CO;2

Poe, S., Nieto-Montes de Oca, A., Torres-Carvajal, O., de Queiroz, K., Velasco, J.A., Truett, B., Gray, L.N., Ryan, M.J., Köhler, G., Ayala-Varela, F. & Latella, I. (2017) A phylogenetic, biogeographic, and taxonomic study of all extant species of *Anolis*

(Squamata; Iguanidae). *Systematic Biology*, 66 (5), 663–697.
https://doi.org/10.1093/sysbio/syx029

Rodríguez Schettino, L. (1999) Systematic accounts of the species. *In:* Rodríguez Schettino, L. (Ed.), *The Iguanid Lizards of Cuba*. The University Press of Florida, Gainesville, Florida, pp. 104–380.

Rodríguez Schettino, L., Losos, J.B., Hertz, P.E., de Queiroz, K., Chamizo, A.R., Leal, M. & Rivalta González, V. (2010) The anoles of Soroa: aspects of their ecological relationships. *Breviora*, 520, 1–22. [The supplementary material contains the previously unpublished manuscript Rand, A.S. & Williams, E.E. The anoles of Soroa.]
https://doi.org/10.3099/0006-9698-520.1.1

Rolfe, S., Pieper, S., Porto, A., Diamond, K., Winchester, J., Shan, S., Kirveslahti, H., Boyer, D., Summers, A. & Maga, A.M. (2021) SlicerMorph: An open and extensible platform to retrieve, visualize and analyze 3D morphology. *Methods in Ecology and Evolution*, 12 (10), 1816–1825.
https://doi.org/10.1111/2041-210X.13669

Ronquist, F., Teslenko, M., van der Mark, P., Ayres, D., Darling, A., Höhna, S., Larget, B., Liu, L., Suchard, M.A. & Huelsenbeck, J.P. (2012) MrBayes 3.2: efficient Bayesian phylogenetic inference and model choice across a large model space. *Systematic Biology*, 61, 539–542.
https://doi.org/10.1093/sysbio/sys029

Ruibal, R. (1964) An annotated checklist and key to the anoline lizards of Cuba. *Bulletin of the Museum of Comparative Zoology, Harvard University*, 130 (8), 473–520. [https://biostor.org/reference/73790]

Sabaj, M.H. (2020) Codes for natural history collections in ichthyology and herpetology. *Copeia*, 108 (3), 593–669.
https://doi.org/10.1643/ASIHCODONS2020

Sanger, T.J., Sherratt, E., McGlothlin, J.W., Brodie, E.D., Losos, J.B. & Abzhanov, A. (2013) Convergent evolution of sexual dimorphism in skull shape using distinct developmental strategies. *Evolution*, 67(8), 2180–2193.
https://doi.org/10.1111/evo.12100

Savage, J.M. & Talbot, J.J. (1978) The giant anoline lizards of Costa Rica and western Panama. *Copeia*, 1978, 480–492.
https://doi.org/10.2307/1443615

Schaad, E.W. & Poe, S. (2010) Patterns of ecomorphological convergence among mainland and island *Anolis* lizards, *Biological Journal of the Linnean Society*, 101 (4), 852–859.
https://doi.org/10.1111/j.1095-8312.2010.01538.x

Underwood, L.M. (1905) A summary of Charles Wright's explorations in Cuba. *Bulletin of the Torrey Botanical Club*, 32 (6), 291–300.
https://doi.org/10.2307/2478811

Williams, E.E. (1969) The ecology of colonization as seen in the zoogeography of anoline lizards on small islands. *The Quarterly Review of Biology*, 44 (4), 345–389.
https://doi.org/10.1086/406245

Williams, E.E. (1995) IV. The morphological characters used in the ANOLEKEY described, defined, and illustrated. *In*: Williams, E.E., Rand, H., Rand, A.S. & O'Hara, R.J. (1995) A computer approach to the comparison and identification of species in difficult taxonomic groups. *Breviora*, 502, pp. 15–37. [https://biostor.org/reference/4052]

Williams, E.E. & Rand, A.S. (1969) *Anolis insolitus*, a new dwarf anole of zoogeographic importance from the mountains of the Dominican Republic. *Breviora*, 326, 1–21. [https://biostor.org/reference/4214]